LAWRENCE
LIVERMORE
NATIONAL
LABORATORY

LLNL-CONF-666247

Archimedean Sprial Antenna With An Integrated Dual Bandstop Response

J. H. Jeon, J. T. Chang, A. Pham

January 21, 2015

2015 IEEE International Symposium on Antennas and Propagation
Vancouver, Canada
July 19, 2015 through July 25, 2015

Disclaimer

Archimedean Spiral Antenna With An Integrated Dual Bandstop Response

Jae H. Jeon, John T. Chang
Lawrence Livermore National Laboratory
Livermore, CA
jeon2@llnl.gov, chang16@llnl.gov

Anh-Vu Pham
Department of Electrical and Computer Engineering
University of California Davis
Davis, CA
pham@ece.ucdavis.edu

***Abstract*—An ultra-wideband Archimedean spiral antenna with an integrated notch filter response at 3.4 GHz and 5.5 GHz is presented. Two pairs of resonant parallel structures are implemented on a generic Archimedean spiral antenna to induce dual stopband characteristics. Measured results on a fabricated antenna prototype experimentally confirm simulation results.**

I. INTRODUCTION

The federal communications commission has allocated 3.1-10.6 GHz for unlicensed uses by ultra-wideband (UWB) systems [1]. The designated spectrum is shared by a number of narrowband wireless standards such as the IEEE 802.11a, satellite communication, and Wi-MAX. Systems employing such narrow band schemes can potentially introduce interference to UWB systems in close proximity.

Antennas based on spiral geometry are able to feature broadband performance due to its frequency independent characteristics [2]. Therefore a generic spiral antenna can be readily designed to operate over the UWB spectrum. Addition of a pair of resonant parallel strips (RPS) to a spiral antenna can induce a bandstop filter response [3]. Integrating a filter response into antennas is a cost-effective and space-saving method to address the interference issue, in comparison to adding an external component filter.

In this paper, an Archimedean spiral antenna with a dual bandstop responses is presented. A pair of RPS induces a single first-order bandstop response. Demonstration of multiple resonant parallel structures inducing multiple bandstop responses is detailed in the following sections.

II. ANTENNA DESCRIPTION

First step in the design process is creating a generic spiral antenna that sufficiently covers the UWB spectrum. A point on an Archimedean spiral is characterized by a linear correlation between its radial distance and azimuth angle [4]. The linear factor can be treated as the expansion rate which is controlled by the inner and outer radius of the spiral and the number of turns. The center feed region is tapered to match the balun transformer width. The end of the spirals is tapered for smooth impedance transition.

A pair of partial spirals that are parallel to the main spirals on the opposite side of the substrate induces a bandstop response [3]. The length and the placement of the RPS determine the bandwidth and center frequency of the stopband. Additional pairs of RPS can be added to induce additional stopbands as long as a finite gap separates adjacent RPSs.

Rogers Duroid 5880 material is used for fabrication. The thickness chosen is 0.79 mm. The final outer radius is at 30 mm. The inner radius is kept at 1 mm. The feed region tapers and narrows to 0.8 mm separation to accommodate a balun of the same thickness as the antenna substrate. The final number of turns chosen is 7. Frequency specificity increases as the number of turns increase. Since two frequency bands are targeted to be notch filtered, it is advantageous to have greatest resolution possible especially in the case where the two notch frequencies of interest are in close spectral proximity. The upper limit is set by the chosen via size at 0.8 mm in diameter, which corresponds to the number of turns at 7. With the given set of design parameters, the optimal placement of the RPS for the Wi-Fi band is found to be at 1.325 turns on the spiral. In this design, the location of RPS refers to edge closer to the outer perimeter. The length of RPS is at 9.5 mm. For the WiMAX band, RPS at 2.33 turns with the length of 15.63 mm provids optimal notch response. Fig. 1 contains the pictures of the fabricated prototype.

Fig. 1. Layout of the PESA with the secondary resonant structure (*Left*), and a picture of the constructed initial prototype (*Right*).

III. RESULTS AND DISCUSSION

Fig. 2 compares the final design in the simulation environment with and without the RPS structures for both bands. The generic design, as expected, shows a very flat VSWR curve. It is below 2:1 from 2.2 GHz all the way to 12 GHz. The integrated notch filter design has peak notch frequencies at 3.4 GHz and 5.63 GHz. VSWR reaches 12:1 for the WiMAX and 16:1 for the Wi-Fi band. For the WiMAX, 2:1 boundary spans from 3.1 to 3.6 GHz and 5.15 to 5.95 GHz for

the Wi-Fi. Flat VSWR profile, less than 2:1, is observed below, between, and above the notch bands. Fig. 2 also compares the simulation result with the measured result. The measured VSWR curve very closely agrees with the simulation result. For the WiMAX band, the peak VSWR level is at 11.8:1. The peak notch frequency comes very close to the desired location at 3.39 GHz. The 2:1 boundary spans from 3 to 3.5 GHz. For the Wi-Fi band, the peak notch frequency is located at 5.55 GHz. The mismatch level is just over 20:1 VSWR. The 2:1 boundary spans from 5.18 GHz to 5.98 GHz. VSWR falls below 2:1 in all three passbands, and follows closely the VSWR level predicted by the simulation.

Gain curve, shown in Fig. 2, is derived from the S21 measurement. For the WiMAX band, suppression of radiation is clearly observed, reaching -5 dB at 3.39 GHz in the measured data. For the Wi-Fi band, the mmeasured result indicates -12 dB at 5.56 GHz in comparison to -3.5 dB at 5.6 GHz from simulation. Overall profile of the passband gain in the measurement follows the same trend as the simulation result. Gain below the WiMAX band is about 4 dB in average. Gain between the WiMAX and Wi-Fi averages about 4.5 dB for the measured and about 5 dB for the simulated result. For the frequency range above the Wi-Fi band, gain averages to about 6 dB, with a slight increase to 5.5 dB between 7 and 8 GHz and a slight drop to 4.55 dB between 9 and 10 GHz in simulation. Measured gain averages to about 5.5 dB up to 9 GHz and drops to 4 dB and 10 GHz. There is a greater fluctuation seen in the measured result due to errors introduced by the effect of the partial anechoic chamber.

Radiation pattern is measured and plotted in Fig. 3 for both the XZ and YZ plane, following the coordinate shown in Fig. 1. Five representative frequencies are chosen: 2.5 GHz for the lower passband, 3.43 GHz for the WiMAX band, 4.5 GHz for the middle passband, 5.6 GHz for the Wi-Fi band, and 8 GHz for the upper passband. The trend in level of radiation from frequency to frequency is similar in both measurement and simulation. At notch frequencies, 3.43 GHz and 5.6 GHz, the level of radiation is significantly reduced throughout all phi angles in both planes compared to the radiation in the passbands. The asymmetry about the XY plane at phi of 90 degrees is attributed to the physical presence of a balun.

Current density plot of the antenna is shown in Fig. 4. The same five frequencies that were chosen for the radiation pattern were chosen for current density. For the three frequencies that represent passbands, there is no visible concentration of current at either of the two RPSs. However, when 3.4 GHz source signal is fed to the antenna, the outer RPS glows, which is responsible for filtering out the WiMAX band. A high concentration of current is evident, testifying to the resonant behavior of RPS. Likewise, when the source signal at 5.6 GHz is fed to the antenna, the inner RPS, which is responsible for the Wi-Fi band, reacts with high concentration of current. Neither of the RPSs reacts to input signal at each other's frequency.

IV. Conclusion

Successful integration of mmultiple bandstop responses by employing a corresponding number of RPSs onto an Archimedean spiral antenna was demonstrated. A prototype has been designed and fabricated. Measurement result closely agreed with the simulation result.

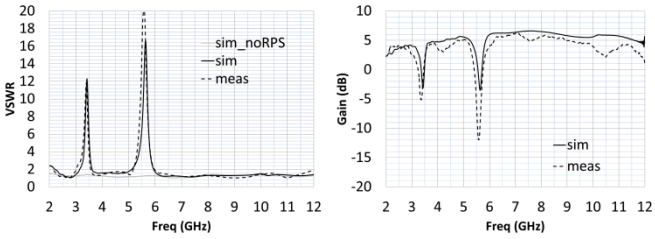

Fig. 2. Simulation (*Solid*) vs. measured (*Dotted*) results: VSWR (*Left)* and Gain (*Right*).

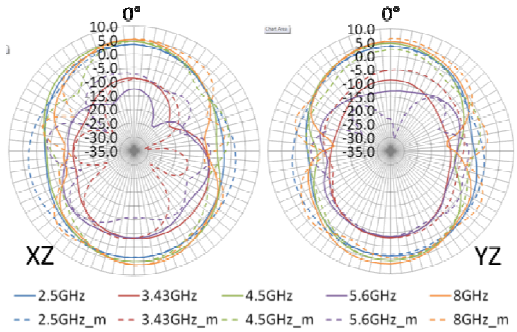

Fig. 3. Radiation pattern from simulation (*Solid*), and measurement of the prototype (*Dashed*) at 2.5 GHz (*Blue*), 3.43 GHz (*Red*), 4.5 GHz (*Green*), 5.63 GHz (*Purple*), and 8 GHz (*Orange*).

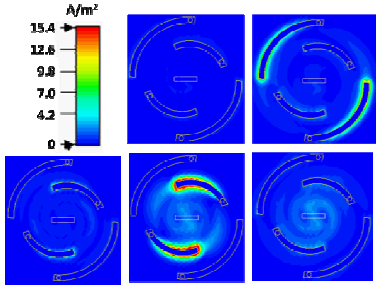

Fig. 4. Intensity plot of current density on RPSs at 2.5 GHz (*Top Middle*), 3.4 GHz (*Top RIght*), 4.5 GHz (*Bottom Left*), 5.6 GHz *(Bottom Middle*), and 8 GHz (*Bottom Right*).

This work was performed under the auspices of the U.S. Department of Energy by Lawrence Livermore National Laboratory under Contract DE-AC52-07NA27344.

References

[1] Federal Communications Commission, "First report and order in the matter of revision of part 15 of the Commission's Rules Regarding Ultra-Wideband Transmission Systems," ET-Docket 98-153, Apr. 22, 2002.

[2] V. H. Rumsey, "Frequency Independent Antennas", 1957 IRE National Convention Record, pp.114 -118 1957.

[3] Jeon, J.H.; Chang, J.T.; Anh-Vu Pham, "Band-notched UWB equiangular spiral antenna," *Antennas and Propagation Society International Symposium (APSURSI), 2014 IEEE*, vol., no., pp.1323,1324, 6-11 July 2014.

[4] Kaiser, J., "The Archimedean two-wire spiral antenna," Antennas and Propagation, IRE Transactions on , vol.8, no.3, pp.312,323, May 1960.